catalysts

MDPI

Review

Review of CO_2 Adsorption Materials and Utilization Technology

Furao Ren and Weijun Liu *

School of Mechanical and Automotive Engineering, Shanghai University of Engineering Science, Shanghai 201620, China; rfr15729259651@163.com
* Correspondence: m310121511@sues.edu.cn

Abstract: This article introduces the recent research status of CO_2 adsorption materials and effective ways of CO_2 resource utilization. Molecular sieves have the advantages of a large specific surface area, a wide pore size range, recyclability, and good chemical and thermal stability. Metal–organic frameworks have diverse structures and broad application prospects. The captured CO_2 is converted into valuable chemicals such as acids, alcohols, hydrocarbons, and esters as raw materials. The rapid development of biomass energy utilization of CO_2, with strong biological adaptability, high yield, low production cost, and low pollutant emissions, is a feasible method to reduce CO_2 emissions. This article analyzes the current research status of CO_2 capture, conversion into chemicals, biomass energy, and industrial utilization from the perspective of catalytic conversion.

Keywords: carbon dioxide; adsorption; reutilization; chemicals; biomass

1. Introduction

The current structure of the energy system maintains high levels of CO_2 emissions. CO_2 emissions are concentrated in the power, steel, and cement industries [1]. CO_2 is the main greenhouse gas. Large-scale CO_2 capture and utilization use CCUS (Carbon Capture, Utilization, and Storage) technology. CCUS refers to the capture and separation of CO_2 from emission sources such as energy utilization, industrial production, or air, and then CO_2 is transported to suitable sites for utilization or storage through tankers, pipelines, ships, etc. [2]. In CCUS, Carbon Capture and Utilization is a CO_2 emission reduction and utilization concept with high application potential [3]. It generates more products with certain economic benefits, thereby compensating for the costs consumed in the CO_2 capture process. CO_2 capture refers to the process of separating and enriching CO_2 from different emission sources through absorption, adsorption, membrane separation, and oxygen-rich combustion. Utilizing CO_2 has become the key to solving environmental and ecological problems. There have been many experimental studies on the application of CO_2 in the fields of biology and chemical engineering. For example, using CO_2 to synthesize biofuels, chemicals, and other high-value-added products. Research includes the catalytic conversion, electrochemical reduction, and other chemical reactions of CO_2, as well as related catalysts and reaction conditions. These research directions cover multiple aspects of CO_2 in the fields of biology and chemistry. It is of great significance for understanding the cycle, transformation, and environmental impact of CO_2, as well as developing new technologies and products for utilizing CO_2.

Because carbon in CO_2 molecules is in the highest oxidation state, their molecules have thermodynamic and kinetic inertness. People are constantly exploring new reaction pathways for effective resource utilization of CO_2 [4]. This article introduces two common materials for CO_2 adsorption and the research progress on CO_2 utilization in chemical engineering, biology, and industrial production fields.

check for updates

Citation: Ren, F.; Liu, W. Review of CO_2 Adsorption Materials and Utilization Technology. *Catalysts* **2023**, *13*, 1176. https://doi.org/10.3390/catal13081176

Academic Editor: Young Dok Kim

Received: 26 June 2023
Revised: 27 July 2023
Accepted: 28 July 2023
Published: 1 August 2023

Copyright: © 2023 by the authors. Licensee MDPI, Basel, Switzerland. This article is an open access article distributed under the terms and conditions of the Creative Commons Attribution (CC BY) license (https://creativecommons.org/licenses/by/4.0/).

2. CO_2 Adsorption Material

The adsorption method utilizes the difference in adsorption capacity of adsorption materials for different gases to capture CO_2. Table 1 shows the applicable conditions, advantages, and disadvantages of different CO_2 capture methods.

Table 1. Main CO_2 capture technologies and relevant advantages/disadvantages [5,6].

Technology Type	Capture Agent	Condition	Gas	Advantage	Disadvantage
Chemical absorption	NH_3	15–27 °C	CO_2/N_2	High CO_2 load capacity	High volatility
	Ionic liquid	Normal atmospheric temperature	CO_2/N_2	Low regeneration energy consumption	Low production rate, high cost
	MOF	High pressure low temperature	CO_2/CH_4, CO_2/H_2	High specific surface area, rich pore structure	High cost, unclear regeneration mechanism
Physical adsorption	Molecular sieve	0–100 °C	CO_2/N_2	Fast adsorption speed, high CO_2 capacity	High pre-treatment cost, poor high-temperature performance
Membrane separation	Glass, rubber	0–60 °C	CO_2/CH_4	High selectivity, easy installation	Poor stability when the mixture is complex
Oxygen-enriched combustion		1000–1500 °C		High CO_2 concentration, high combustion efficiency	High energy consumption High equipment requirements High process complexity

2.1. Molecular Sieve

A molecular sieve refers to a material with pores and a skeletal structure that can be used as a catalyst. The crystalline state of molecular sieves is silicate or silicon aluminate. When the reactant enters the molecular sieve, a catalytic reaction occurs. At the end of the reaction, the product flows out of the molecular sieve pores. Molecular sieves have various characteristics. Molecular sieves have adjustable pore sizes [4]. The pore size of molecular sieves can be controlled by adjusting the synthesis conditions, ranging from nanoscale to microscale [7]. Therefore, appropriate pore sizes can be selected according to needs. Molecular sieves have a high specific surface area and provide a large number of active surfaces, which are conducive to reactions such as adsorption and catalysis. Molecular sieves have adsorption selectivity [8]. Its pore size and pore structure selectively adsorb certain molecules or substances within the molecular size range. Molecular sieves have high thermal stability and maintain their structure and performance without significant changes at high temperatures [9]. Molecular sieves have high chemical stability [10]. They maintain their structure and properties without being damaged under strongly acidic or alkaline conditions. The preparation methods of molecular sieves include hydrothermal synthesis, hydrothermal conversion, microwave technology, ion exchange, nanotechnology, etc. Common methods for modifying molecular sieves include cation exchange [11–13], such as Cu^{2+} and Ni^{2+}; the functional group introduction method, which improves pore size [14–16], such as amino groups; and element-doping methods [17], such as silver and titanium. The impregnation method improves adsorption selectivity, and molecular sieves are loaded with metals such as Zn [18].

2.1.1. Molecular Sieve Classification

According to elements, molecular sieves are divided into silicon aluminum type, silicon type, oxygen type, and carbon nanotubes. A silicon aluminum molecular sieve is a network structure formed by sharing oxygen atoms between silicon oxygen tetrahedra and aluminum oxygen tetrahedra, such as Zeolite A and Zeolite X. Silicon-type molecular sieves have a network structure composed of silica tetrahedra, such as MCM-41, MCM-48, etc. Oxygen-type molecular sieves have a network structure composed of oxygen tetrahedra, such as AlPO4, SAPO-34, etc. Carbon nanotubes are tubular structures composed of carbon atoms. According to the pore size, molecular sieves are divided into microporous molecular sieves (<2 nm), mesoporous molecular sieves (2–50 nm), and macroporous molecular sieves (>50 nm). According to the silicon/aluminum ratio, molecular sieves can be divided into A-type, X-type, and Y-type [19]. Different types of molecular sieves are shown in Figure 1 [19].

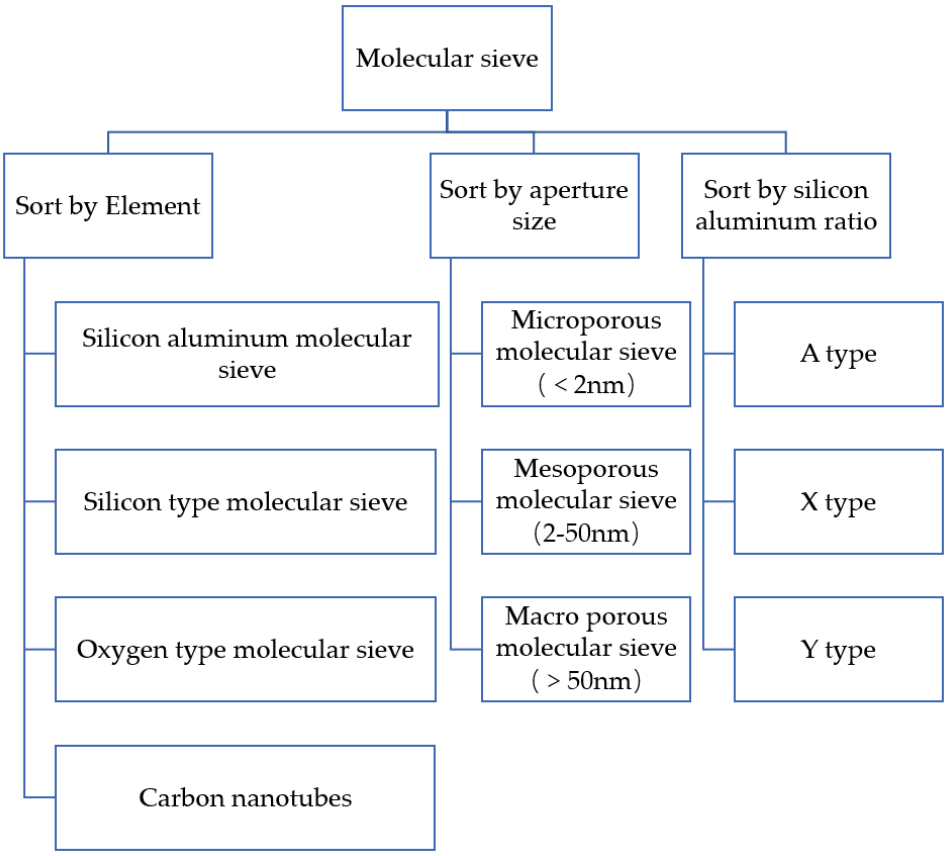


Figure 1. Molecular sieve classification [19].

2.1.2. Effect of Cationic Modification on the Adsorption Performance of Adsorbents

The displacement of cations in molecular sieves regulates their acidity and alkalinity [11]. Aluminum in molecular sieves is a cation, and cations are acidic sites. The skeleton oxygen closest to the cation provides a pair of alkaline sites for each cation. Therefore, the alkalinity of molecular sieves increases with the increase in aluminum content in the skeleton [12]. The order of adsorption capacity of each cation for CO_2 is $Li^+ > Na^+ > K^+ > Cu^+$ [20]. For different zeolites with the same cation, the adsorption capacity of Li exchange molecular sieves decreases in the order Y > A > ZSM-5. In the Y zeolite exchanged with divalent metal cations, the adsorption capacity of CO_2 decreases in the order of $Mg^{2+} > Ca^{2+} > Be^{2+} > Zn^{2+}$. The adsorption capacity of alkali metal ions varies at different sites [21]. The structures where Li^+ and Na^+ fall on S6R and K^+ fall on S8R have good adsorption advantages. The X molecular sieve is an octahedral zeolite molecular sieve (FAU) with the chemical formula $M_{86}Al_{86}Si_{10}$. M represents cations such as Li^+, Na^+, K^+, etc. In molecular sieves, CO_2 and cation M skeleton oxygen atoms Oz form an adsorbent structure with M-O=C=O⊥Oz. Yang Kaizhong et al. [22] found that the M-O distance of the adsorption structure in molecular sieves meets the requirements of LiX < NaX < KX, and the simulated adsorption amount of CO_2 meets the requirements of LiX > NaX > KX. Different cations affect the M-O distance in the molecular sieve adsorption structure to affect the structural energy of the adsorbent, thereby affecting its CO_2 adsorption capacity. Feng et al. [13] synthesized Na-SSZ-13 molecular sieves by the hydrothermal method.

Alkali metal cations are located at three different sites in SSZ-13. There are 2 sites in each crystal cell at the center of the six-membered ring channel (site S II). In an eight-membered ring, there are four sites in each crystal cell near the vertex of the four-membered ring (site S III). Near the center of the eight-membered ring (site S III′), there are two sites in each crystal cell [23]. Ion exchange was carried out on the sample using ammonium nitrate, lithium nitrate, and potassium nitrate. Due to the fact that Na^+ preferentially occupies

the S II and S III sites in the molecular sieve framework, cations located at the S III site in the eight-membered ring preferentially adsorb gas molecules. The behavior of Na^+ preferentially occupying the S III site in the center of the eight-membered ring results in a higher adsorption capacity of Na SSZ-13. Due to the molecular trap gate effect, although the adsorption capacity of K-SSZ-3 is not high, it has excellent adsorption selectivity.

2.1.3. Regulating the Pore Structure of Molecular Sieves

The essence of zeolite molecular sieve adsorption is that substances with a molecular diameter smaller than the pore size of the molecular sieve crystal can enter the molecular sieve crystal and be adsorbed [24]. Siriwardane et al. [25] found that the kinetic diameter of CO_2 is 0.33 nm. The adsorption capacity of a 13X molecular sieve with a larger pore size (about 1 nm) is better than that of a 4A molecular sieve (about 0.4 nm). Gao Junwei et al. [26] simulated the adsorption of CO_2 on FAU. The results indicate that in the saturated state of adsorption, the larger the pore structure of the molecular sieve, the greater the adsorption capacity of CO_2. For microporous structures smaller than CO_2 molecules, adsorption hardly occurs. At low fugacity, CO_2 adsorption mainly occurs in small pores. At high fugacity, the increase in adsorption capacity mainly occurs within the macropores. The adsorption process of CO_2 on the FAU molecular sieve conforms to the type I Langmuir adsorption isotherm. The adsorption capacity of adsorbents for CO_2 under high pressure is much greater than that under low pressure.

An adsorption material with high CO_2 adsorption capacity requires the presence of well-developed micropores and a large number of narrow micropores [14]. Two-step crystallization is beneficial for the generation of multi-level pore structures, and the introduction of amino acids helps to improve the relative crystallinity and yield of molecular sieves [27]. Ma Yanhui et al. [28] used a two-step crystallization method to assemble and synthesize microporous and mesoporous composite molecular sieves. The adsorption capacity of this material for CO_2 is significantly improved compared to pure microporous or mesoporous materials. The maximum CO_2 adsorption capacity of P-ZSM-MCM41 reaches 1.51 $mmol \cdot g^{-1}$, which is more than twice the adsorption capacity of ZSM-5 zeolite.

The introduction of special molecular groups such as amino and organic amines into molecular sieves can improve the adsorption capacity of CO_2. Wu Wei et al. [15] prepared CO_2 adsorption materials by loading modified organic amines into the pores of irregular molecular sieves through the impregnation method. Under the same conditions, DMS-P1, with a larger surface area and pore volume, has good CO_2 adsorption performance and cycling stability. Hani [16] adjusted the pore properties of zeolite imidazolium salt frameworks (ZIFs) to improve their gas adsorption performance, and used cationic dyes such as rhodamine B and methylene blue to synthesize porous ZIF-8 (Dye@ZIF-8). Under the same conditions, its CO_2 adsorption capacity increased by 42% compared to ZIF-8 (0.84 $mmol \cdot g^{-1}$). The presence of dye molecules enhances the adsorption capacity of ZIF-8 crystals for CO_2.

A larger pore size makes it easier for CO_2 molecules to pass through, making adsorption more likely to occur. In pores smaller than CO_2 molecules, adsorption hardly occurs. Different shapes of pores will have different effects on the orientation and interaction of CO_2 molecules, thereby affecting the adsorption capacity and selectivity of CO_2. The surface properties also affect the adsorption capacity of CO_2. Special surface functional groups undergo chemical reactions or electrostatic interactions with CO_2 molecules, thereby increasing adsorption capacity and selectivity.

2.1.4. Preparation of Molecular Sieves Using Biomass Materials

The biomass used to make molecular sieves includes wood waste, crop waste such as rice husks, cellulose waste such as pulp residue, etc. Extracting residue from sunflower seeds for zinc chloride activation aims to improve the adsorption capacity of the adsorbent and increase the yield of carbon molecular sieve products. Taguchi design is a commonly used quality design method that reduces product design and manufacturing risks through

systematic methods, improving product quality, reliability, and stability. The Taguchi method is a powerful tool for simultaneously optimizing the adsorption capacity of adsorbents and improving the yield of carbon molecular sieves [29]. Ugur M [29] used the Taguchi design method to prepare carbon molecular sieves by chemical vapor deposition of methane on activated carbon. The optimal synthesis conditions not only provide the maximum CO_2 adsorption capacity, but also improve the adsorbent yield. The Taguchi design method is helpful for the controllable adsorption of CO_2 by carbon molecular sieves and is expected to become a useful method for the preparation conditions of carbon molecular sieves.

Molecular sieves prepared from biomass waste may have a lower specific surface area and simpler pore structure compared to traditional synthesis methods. However, due to the abundant sources and low cost of biomass waste, the preparation of molecular sieves from biomass waste has important environmental and economic significance.

2.2. Metal–Organic Frameworks

Metal–organic frameworks (MOFs), also known as porous coordination polymers (PCPs), are assembled by metal ions and organic ligands, becoming a new class of crystalline porous materials [30]. The ease of design, fine-tuning, and uniform pore structure make them promising materials for various applications. In gas absorption, the number of adsorption sites of MOFs has a significant impact on their absorption capacity. Multisite MOFs contain multiple gas adsorption sites, which can enhance gas adsorption capacity. The CO_2 adsorption in MOFs is divided into two parts, namely high-pressure adsorption and selective adsorption at approximately atmospheric pressure. The pore volume affects the adsorption of MOFs at high pressure, and the adsorption heat affects the adsorption of MOFs at low pressure [31].

Due to the diversity of metal ions and organic ligands, there are various types of MOF materials, mainly including network metal–organic framework materials (IRMOFs), zeolite-like imidazole ester framework materials (ZIFs), Lavasher framework materials (MILs), University of Oslo framework materials (UiO), porous coordination network structural materials (PCN), and pillar-supported metal–organic framework materials (CPL) [32].

The modification methods of MOF materials include introducing functional groups, doping metal ions, and preparing composite materials. The adsorption capacity of different MOF materials is shown in Table 2.

Table 2. The specific surface and CO_2 adsorption values of different materials.

Type	Specific Surface Area ($m^2 \cdot g^{-1}$)	CO_2 Adsorption Capacity	Temperature/k	Pressure/bar	Reference
IRMOF-11	2096	14.7 $mmol \cdot g^{-1}$	298	30	[33]
HKUST-1	1781	10.7 $mmol \cdot g^{-1}$	298	35	[34]
IRMOF-1	2833	21.7 $mmol \cdot g^{-1}$	298	35	[34]
MOF-177	4508	33.5 $mmol \cdot g^{-1}$	298	35	[34]
MIL-100(Cr)	1900	280 $cm^3 \cdot cm^{-3}$	303	50	[34]
MIL-101(Cr)	4230	390 $cm^3 \cdot cm^{-3}$	303	50	[34]
MOF-200	4530	54.5 $cm^3 \cdot cm^{-3}$	298	50	[35]
MOF-201	6240	54.5 $cm^3 \cdot cm^{-3}$	298	50	[35]

2.2.1. Introducing Functional Groups

Introducing special functional groups on the existing MOF template significantly improves the adsorption capacity and selectivity of the adsorbent, with the introduction of amino groups being a common occurrence. Meng Liuli [36] synthesized an amino-functionalized column layer MOF-SNNNU-Bai65 using a new ligand. Compared with the prototype SYSU, the functional modification of the pore surface by amino groups and the segmentation of pore channels enable SNNU-Bai65 to exhibit better adsorption and separation of CO_2/N_2 and CO_2/CH_4 after activation.

In addition to amino modification methods, introducing amine functional groups is also a common method. Planas [37] and others observed the stoichiometry of 2:2-amine: CO_2 of this material through amination MOFs, which has a higher adsorption capacity and weaker CO_2 binding energy than the 2:1 stoichiometry observed in most amine-functionalized adsorbents. Liu Qiwei [38] successfully introduced PEI molecules into the AlFu framework by modifying aluminum fumaric acid MOFs (AlFu) with polyethylene imine (PEI) through the impregnation method. The loading of PEI molecules will not damage the lattice structure of the AlFu skeleton. An increase in PEI loading will lead to the aggregation of the AlFu skeleton, resulting in a decrease in the specific surface area and pore volume of the material. The amine-lined pores provide high values for the surface area and adsorption heat of MOFs [39]. Wei Meng et al. [40] synthesized three Co-based MOF-74-III materials with extended pores. The material exhibits varying degrees of condensed benzene rings on the same length of ligand side chains. The fusion of the benzene ring and ligand hinders the function of the CoII center as a Lewis acid site. The adsorption of CO_2 by the adsorbent and the selectivity of CO_2/CH_4 and CO_2/N_2 are significantly improved.

In addition, there are composite materials formed by the complexation of chemically modified MOFs. Guangdong Yang [41] synthesized a composite material composed of amine-functionalized imidazole-type poly (PIL) and MOFs. Thanks to the large surface area of MOFs and the high CO_2 diffusion rate of ionic liquids, the synthesized composite material achieved a CO_2 adsorption capacity of 19.5 $cm^3 \cdot g^{-1}$ at a CO_2 partial pressure of 0.2 bar and 25 °C. MOF materials exhibit lower CO_2 adsorption and stability performances in humid environments. Wang Xiaoguang [42] used chemical modification to carboxylate multi-walled carbon nanotubes (MWCNT, multi-walled carbon nanotube) and synthesized multi-walled carbon nanotubes/Mg-MOF-74 composite materials using the solvothermal method (CNT@Mg-MOF-74). The doping of MWCNTs does not affect the structure and morphology of Mg-MOF-74. CNT@Mg-MOF-74 has better hydrophobic capacity and structural stability in humid environments.

Park et al. [43] synthesized a photothermal switchable MOF using the ligand 2-phenyldiazenyl terephthalate. The form of ligand acids changes from trans to cis through photochemical means and from cis to trans through thermal means. The obtained MOF adsorbs different amounts of CO_2 after light irradiation or heat treatment.

2.2.2. Doped Metal Ions

Metal ions have specific requirements for geometric coordination and oxidation states, and different metal ions can produce different skeletal structures. The doped metal ions react with uncoordinated oxygen-containing groups in the skeleton material, replacing the proton H in -OH to form metal O coordination, thereby forming new CO_2 adsorption sites and enhancing the electrostatic interaction between the material and CO_2 [44]. The main methods for doping metal ions include the condensation reflux method, the hot solvent method, etc. Cheng Yan [45] synthesized MOF-74 materials with Co, Ni, Ce, Zn, and Cu as metal center ions using the condensation reflux method. There are a large number of unsaturated Ni^{2+} metal sites in the micropores of synthetic materials, and Ni^{2+} interacts strongly with CO_2.The specific surface area of MOF-74 (Ni) is 1128.61 $m^2 \cdot g^{-1}$, and the CO_2 adsorption capacity is 6.8 $mmol \cdot g^{-1}$, which is much higher than other adsorbents. Hua et al. prepared Li @ HKUST-1 by doping Li^+ onto HKUST-1, with a Li/Cu ratio of 0.07. The modified HKUST-1 increased the adsorption capacity by 59%. This can be attributed to the strong electrostatic interaction between Li^+ and CO_2 [46].

Anion column hybrid MOFs are porous materials that use fluorinated anion groups as support columns [47]. LIU X et al. found that AP-MOF materials with interpenetrating structures are beneficial for CO_2 adsorption, while AP-MOFs with non-interpenetrating structures are beneficial for CO_2/N_2 separation [48].

The introduction of metal ions increases the active site and charge distribution of MOFs and improves the adsorption capacity and selectivity of CO_2. In addition, metal ions regulate the pore size and shape of MOFs, further optimizing CO_2 adsorption performance.

2.2.3. Composite Materials Made by Combining MOFs with Functional Materials

In order to improve the catalytic performance and mechanical strength of MOFs, they are combined with functional materials such as metal nanoions and enzymes. Nguyen [49] synthesized a microporous copper-based Cu_2 (ABTC) (ABTC = 3,3′,5,5′-azophenyltetracarboxylic acid). It has open Cu sites, accessible pore cage structures, hexagonal channels, permanent porosities, a BET surface area of 2200 $m^2 \cdot g^{-1}$, and good low-pressure CO_2 absorption. At 298 K, the CO_2 absorption reached 93 $cm^3 \cdot g^{-1}$, with moderate selectivity for CO_2. The catalytic activity of Cu_2 (ABTC) is superior to other Cu MOFs and can be reused up to six times without significant reduction in catalytic activity.

Chen Yongwei [50] selected MOF-505 and graphite oxide (GO) to prepare water vapor-stabilized composites. The increase in dispersion force and unsaturated metal sites is a strategy for improving CO_2 adsorption and separation. The selectivity indices for CO_2/CH_4 and CO_2/N_2 adsorption were 8.6 and 37.2, respectively. MOF-505@GO Compared with MOF-505, the CO_2 adsorption capacity increased by 37.3%, and the CO_2/CH_4 and CO_2/N_2 selectivity increased by 13.2% and 33.8%, respectively.

2.2.4. Other Influencing Factors

Porous metal organic compound (DOBDC, 2,5-dioxido-1,4-benzenedicarboxylate) series MOFs are materials with unsaturated metal centers in their crystal structure, such as Ni/DOBDC and Mg/DOBDC. Due to its high CO_2 capacity below atmospheric pressure, DOBDC serves as an adsorbent for capturing CO_2 from flue gas, but its stability is poor. Liu et al. [32] studied the stability of Ni/DOBDC and Mg/DOBDC. The results indicate that Ni/DOBDC maintains its CO_2 capacity after steam conditioning and long-term storage, while Mg/DOBDC cannot. Introducing water vapor into simulated flue gas will reduce the CO_2 capacity of Ni/DOBDC. Copper-based catalysts have high effectiveness and low economic costs. Hamon et al. [51] found that Cu-BTC has a high delta (difference in adsorption capacity between adsorption and desorption conditions) loading, but low CO_2 gas selectivity. It forms a structure presenting a large pore surrounded by eight small pores called side pockets. During the low-pressure stage, it is difficult for CO_2 molecules to enter the small pores, while the large pores are responsible for the low-pressure area. As the pressure increases, the side pores significantly enhance the CO_2 adsorption capacity, which makes Cu-BTC suitable for pressure swing adsorption. Kim et al. [52] prepared a flexible metal organic skeleton, Cu (II)-TCM, with a non-interpenetrating 3D structure with large pores and void spaces. When activated with supercritical CO_2, Cu (II)-TCM has greater gas adsorption capacity than when activated with the thermal evacuation method and selectively adsorbs CO_2 instead of N_2 at room temperature.

At a pressure of 1 bar, the CO_2 adsorption capacity of each adsorbent is shown in Table 3.

Table 3. CO_2 adsorption performance of each adsorbent.

Type	Temperature/k	CO_2 Adsorption Capacity/mmol·g^{-1}	Source
P-ZSM-MCM41(2)	273	1.51	[25]
Multistage NaX	273	6.8839	[26]
JLOX-500		4.02	[53]
carbon molecular sieve	273	2.6228	[29]
NaY	298	3.74	[54]
ZIF	298	1.1116	[55]
APTES molecular sieve		1.44	[56]
Mg-MOF-74	298	1.358	[38]
CNT@MgMOF-74	298	1.8155	[42]

Table 3. *Cont.*

Type	Temperature/k	CO_2 Adsorption Capacity/mmol·g^{-1}	Source
MOF-74(Ni)-24-140	273 298	8.29 6.61	[49]
MOF-74(Ni)		6.8	[49]
CoFe-MOF-74		2.9243	[50]
(MOF)Cu_2(ABTC)	298	4.1517	[51]
MIL-101(Cr)-NH_2	278	5.4	[57]
MIL-101(Cr)	298	1.3396	[58]
MOF-505@GO	298	3.94	[50]
NH_2-MIL-101(Cr)	273 298	2.3 1.6	[59]

3. Utilization of CO_2

CO_2 capture and utilization technology has been applied in different fields. Globally, technologies such as CO_2 to chemicals, fuel production, microalgae carbon sequestration, enhanced oil recovery rate (EOR), biomass energy, and improved planting have been applied [60]. It is estimated that by 2050, 6.2 billion tons of carbon dioxide will be captured and utilized through three pathways: concrete, chemistry, and minerals [61].

3.1. Using CO_2 as a Raw Material to Produce Chemicals

In various applications of organic synthesis, CO_2 can be used as a raw material for fuel production. Transforming CO_2 into organic small molecules through catalysis not only reduces CO_2 concentration but also addresses two major challenges in the future, namely climate change and the production of alternative fuels [62]. The conversion of CO_2 into CH_3OH, HCOOH, and CH_2O- has become the main research field. The excitation methods for catalysts required for reaction occurrence include photoenergy, electrocatalysis, and thermal catalysis. Exciting the catalyst with light energy directly utilizes renewable energy, such as solar energy. It has high selectivity and reaction efficiency. The disadvantage is that the stability and activity of the catalyst are easily affected by light intensity and wavelength. The high efficiency of electrocatalytic catalysis, combined with renewable energy, has the disadvantage that the stability and activity of the catalyst are easily affected by current density and electrolyte composition. At the same time, it is necessary to solve the problems of catalyst regeneration and recovery. The thermal catalytic method has the advantages of high stability and activity of the catalyst, but low selectivity and reaction efficiency require a large amount of energy input.

3.1.1. Acid Production Using CO_2 as a Raw Material

Formic acid is an ideal chemical hydrogen storage medium and a promising fuel source. CO_2 hydrogenation to formic acid has a high atom economy and is one of the most effective ways to reduce CO_2 emissions. In the catalytic hydrogenation of CO_2 to formic acid using Ag single-atom-supported N-modified graphene, the introduction of N enhances the catalyst's adsorption capacity for reactants, reduces the reaction activation energy, and improves the catalytic activity of the catalyst. This provides a theoretical basis for the new 2D catalyst to catalyze CO_2 hydrogenation to formic acid [63].

The CuO-FS catalyst prepared by Guo Lina et al. [64] improved the activity of electroreduction of CO_2 and the selectivity of the reduction product, formic acid. The reaction mechanism shows that the excellent electrochemical reduction performance of CuO-FS is attributed to its greater electrochemical activity. The surface area provides a large number of active sites, resulting in a higher total current density. During the electrocatalytic process, less zero-valent Cu is generated on the catalyst surface, reducing the generation of ethylene and making the product more concentrated in formic acid. He Jiehong [65] prepared an amorphous NiRu0.1B catalyst for the hydrogenation of CO_2 to fatty acids (FA). The amor-

phous structure of the catalyst provides abundant dangling bonds and unsaturated atoms for enhancing the gas adsorption of reactants. Due to the synergistic effect of amorphous structure and electron donation, the amorphous NiRu0.1B catalyst exhibits higher activity and stability at low temperatures compared to Ni B and crystalline Ni B. Asare et al. [66] produce advanced carboxylic acids using polyols, CO_2, and H_2 as raw materials. In a binary solvent of ionic liquid (1-butyl-3-methylimidazolium iodide salt) and water, the Rh catalyst effectively increases the reaction rate, with cheap and non-toxic I_2 as the promoter. The reaction can be carried out above 100 °C. Under optimal conditions, the yield of carboxylic acid can reach as high as 86.4%.

The conversion of CO_2 into fuel driven by sunlight is a solution to the storage of renewable energy. Zhao Jiwu et al. [67] studied an entire solar-powered artificial photosynthetic system (APS). The system adjusts the photovoltaic photoelectron chemical cell to efficiently produce formic acid fuel from CO_2 and H_2O under unpolarized lighting. The BiOI-Bi (BOI-Bi) cathode catalyst has high selectivity for the conversion of CO_2 to HCOOH. The APS has high product selectivity, strong activity, and good durability.

3.1.2. Ethanol Production Using CO_2 as a Raw Material

CH_3OH is a liquid fuel that is easy to store and transport and is also a raw material for many chemicals [68]. Methanol can be converted into hydrogen-rich gas, which can be fed into fuel cells to generate electricity [69]. Converting CO_2 into methanol is a favorable way to solve the problems of CO_2 emissions and energy scarcity.

Koh [70] dispersed metal components Cu, Zn, and Mn on mesoporous molecular sieve SBA-15 using the citric acid impregnation method, creating rich Cu sites for H_2 adsorption on CZM/SBA15. In the presence of abundant hydrogen species, a strong reducing microenvironment is formed, which is conducive to CO_2 hydrogenation to methanol. The interaction between new catalysts and renewable energy can also achieve good CO_2 conversion effects [71]. Chang Fei et al. [57] reduced CO_2 to methanol using ionic liquids. The process of reducing CO_2 to methanol using ionic liquids has both economic benefits and the potential for carbon reduction. Under the best assumption, the new process can reduce costs by approximately 11.67%. Compared with the traditional coal-to-methanol process, 3.85 kg of CO_2 is emitted for every 1 kg of methanol produced. The highest carbon emissions from producing 1 kg of methanol are −1.08 kg CO_2 (for photovoltaic power generation) and −1.29 kg CO_2 (for nuclear/wind power) [72]. If renewable energy is fully used to provide electricity, negative carbon emissions within the life cycle can be achieved, which means that a maximum of 1.29 kg of CO_2 can be consumed for every 1 kg of methanol produced. This means that it does not emit additional CO_2 into the environment and also absorbs more CO_2. Izadpanah [58] modified the original ZIF-8 with ZnO, Pt, Cu, and Au nanoparticles (NPs) to obtain four new photocatalysts for reducing CO_2 to methanol under UV/Vis light irradiation at room temperature. The characteristic of the ZnO/ZIF-8 photocatalyst is the permanent generation of oxygen vacancies and electron hole pairs in ZnO NPs, as well as the formation of type II heterojunctions, resulting in effective charge carrier separation and a higher methanol yield. In metal NPs, Pt/ZIF-8 samples have higher light capture ability and a larger surface area, which can provide more effective interaction between CO_2 and photocatalysts.

Waste biomass can be used as catalyst raw materials. Tseng I [73] recycled bagasse (SB) for photocatalytic applications loaded with graphite, like carbon nitride (gCN). The gCN loaded on SB converts CO_2 into CO or methanol. The composition of functional groups on the sample can be adjusted through hydrothermal reactions, thereby changing the affinity for CO_2 and improving the conversion efficiency of CO_2.

The additives in the catalyst significantly increase the production of methanol. The addition of Pd improves the dispersion and specific surface area of the catalyst. The strong interaction between Pd and Cu in the catalyst shifts the Cu_2p orbital binding energy to a lower position, reduces the reduction temperature, and improves the CO_2 hydrogenation activity [74]. Wang Hao [74] built a new type of similar Cu@Zr-CeO_2 reverse-phase catalyst.

The catalyst has higher methanol selectivity and spatiotemporal yield. The improvement of catalytic performance is related to the highly dispersed active Cu0 sites, abundant intermediate and strong alkaline sites, good interface Cu^{+} sites, and abundant Zr^{4+}-$OvCe^{3+}$-like defect structures. These surface or interface structures can promote the adsorption and activation of CO_2, accelerate the conversion of formate intermediates, and facilitate the selective generation of methanol through CO_2 hydrogenation. Wang Li [75] studied the effects of Ga on Cu@ZnO and the impact of reduction capacity and CO_2 adsorption capacity. The addition of Ga not only increases the surface area of the catalyst and the contact area between the active component and CO_2, but also helps to increase the dispersity of Cu and the number of total alkaline sites and promote CO_2 adsorption.

Metal CO_2 batteries have great potential for improving the efficiency of CO_2 conversion into fuel. Sukhjot K et al. [76] have fabricated B-, N-containing carbon with tubular morphology (C-BN@600) derived from ionic liquid (IL) and metal-organic framework (MOF) composites. The Faraday efficiency of the catalyst is 74%, with a yield of 2665 μG h^{-1} mg^{-1} cat in electrochemical CO_2 reduction to methanol. Assembled batteries consume carbon dioxide during the discharge process and electrochemically convert it into methanol, while generating electrical energy. The dual goals of CO_2 reduction and energy storage have been achieved.

3.1.3. Ester Production Using CO_2 as a Raw Material

Dimethyl carbonate (DMC) is an important intermediate synthetic material with various reaction properties that can be used to produce various chemical products such as esters and alcohols [77,78]. The direct synthesis of dimethyl carbonate (DMC) from CO_2 and methanol is a sustainable way to produce DMC and utilize CO_2. Yuan Keng et al. [79] prepared MOF-808 using a simple one-pot method, encapsulating phosphotungstic acid (HPW) into a micropore (HPW@MOF-808) medium. The interaction between encapsulated HPW and Zr6 nodes inhibits the leaching of HPW during the reaction process. HPW@MOF-808 has better reusability than HPW/MOF-808. Velpuri V. [80] et al. used mixed metal oxide (CuO ZnO) nanosheets/microsheets (Cozi nmf) to catalyze the conversion of CO_2 to cyclic carbonates at room temperature. Cozi-mf effectively promotes the unobstructed movement of electrons and the adsorption of substrates, and the yield of synthesized cyclic carbonates is above 95%. Cyclic carbonates are synthesized industrially by immobilizing CO_2 with epoxides. The synthesis of cyclic carbonates is a 100% atomic economy reaction, which makes it environmentally friendly and promising. Using tetrabutylammonium bromide (TBAB) as the catalyst, epoxy propane as the mode substrate, and the addition of water significantly increases the yield of propylene carbonate and reduces the activation energy [81].

3.2. Production of Biomass by Combining CO_2 with Biology

Among the methods for utilizing CO_2, the biological carbon sequestration method is more feasible than physical and chemical methods due to its low cost and almost zero emissions of other pollutants. Biological carbon sequestration is mainly manifested in plants, cyanobacteria, and microalgae that fix CO_2 from the atmosphere and use CO_2 as a carbon source for biological growth. Plants and algae absorb CO_2 from the atmosphere through photosynthesis and convert it into organic matter. The CO_2 absorbed through photosynthesis can also be used to produce biomass fuels, such as biodiesel and bioethanol. Compared to the combustion process of fossil fuels, the combustion of biomass fuels produces lower CO_2 emissions, reducing greenhouse gas emissions.

In recent years, microalgae cultivation has attracted great research interest worldwide due to its high growth rate, high CO_2 storage rate, high tolerance to different environmental conditions, and accumulation of high-value-added compounds during the growth stage. The microalgae isolation system is considered a green technology for capturing CO_2, and it can use exhaust gas from industrial flue gas for biomass production. The hybrid system of CO_2 absorption and microalgae conversion (CAMC) can not only overcome the challenge of

high-energy solvent-consuming thermal regeneration in the process of CO_2 absorption but also improve the carbon conversion efficiency in the process of biotransformation [82]. In addition, the biomass of microalgae can be used in the fields of health products, cosmetics, and energy, which can improve the economic feasibility of CO_2 reduction processes based on microalgae [83]. Wiesberg [84] studied the capture of CO_2 by chlorella and then used the biomass energy generated as raw materials for biological refineries (BRY). The results indicate that BRY is more effective at carbon capture than traditional CCS using amines to capture CO_2.

The development of CO_2 fixation mechanism (CAMC) systems is limited due to the incompatibility between CO_2 absorption and biotransformation rate. The cultivation of Chlorella vulgaris strains uses low-temperature plasma (LTP) mutation breeding technology to combine non directed mutagenesis with directed screening [85]. After mutation treatment, the carbon sequestration rate of wild Chlorella L166 increased from 82.9% to 93.7%. In addition, the lipid production of L166-M3 increased to 6.89 $mg{\cdot}L^{-1}$, which is 15.4% higher than that of the original Chlorella L166. LTP mutation breeding can serve as a potential method for cultivating algae species and improving the overall performance of CAMC systems. Jing X et al. [86] studied the CO_2 utilization based on biomass in the iron cycle (BCU-Fe, biomass-based utilization-Fe) system, which converts CO_2 into formate through Fe under hydrothermal conditions and recovers Fe using glycerol derived from biomass. This system serves as a universal tool for guiding the industrialization of emerging carbon neutrality technologies.

Biocarbon sequestration and biomass energy preparation are complex processes that involve multiple links and technologies. Different biomass energy preparation methods and technologies are selected and optimized based on specific biomass and needs.

3.3. CO_2 Promotes Industrial Production

Injecting CO_2 to increase oil well pressure and displace crude oil has become a key technology for improving oil recovery efficiency [87]. During the production of ready-mixed concrete, injecting CO_2 during the batching and mixing process improves the compressive strength of the concrete [88]. In farmland, grassland, and forests, powdery silicate rock reacts with atmospheric CO_2 to mineralize and form carbonate rock. By combining CO_2 with other catalysts, some environmental problems caused by industrial production can be solved. Kang et al. [89] discussed the process of carbon capture and utilization using industrial wastewater. Monoethanolamine (MEA) aqueous solution is used as an absorbent solution. The solution contains calcium ions with a concentration of 21,972.64 ppm, used to provide calcium cations. When a pre-treated saline solution is added to a saturated MEA solution, the captured CO_2 is converted into calcium carbonate through a carbon sequestration process. Most calcium carbonate exists in the form of calcite. In the process of CO_2 flooding, new materials are added by controlling the fluidity of the injected CO_2 during the flow through porous and permeable reservoirs. Shankar et al. [90] used nanoparticles and related additives in the foam flooding scheme. With the addition of SiO_2 (0.1–2 wt%) and TiO_2 (0.1 wt%) nanocomposites, CO_2 foam exhibits temperature resistance and viscoelastic properties of shear thinning. The CO_2 foam stabilized by the nanocomposite shows a total cumulative oil recovery rate of 78% at 40 °C, which is higher than that of the nanocomposite without CO_2 (70%).

The carbonization and solidification of cement-based materials are important for CO_2 utilization and storage. CO_2 mineralization curing improves the low strength and poor durability of recycled concrete aggregates. Zhuo et al. [91] proposed a method to achieve low-carbon cementitious materials and improve their mechanical properties. CO_2 was used to prepare uniformly dispersed $CaCO_3$ suspensions and cement slurry. The compressive strength has increased by 16%. The nucleation effect caused by the high-level dispersion of $CaCO_3$ particles in $CaCO_3$ suspension promotes cement hydration and densifies the microstructure. Most previous studies have focused on pure CO_2 carbonation solidification. Lixi et al. [92] demonstrated the superior CO_2 absorption and enhanced compressive

strength of flue gas (20% CO_2 concentration) during carbonation solidification. At the beginning of solidification, the carbonization rate of the flue gas is small, but at 12 h of carbonization, the CO_2 absorption and compressive strength are greater than those of pure CO_2 solidification. Low concentration CO_2 has a higher carbonization ability in cement carbonization curing, which may open up new avenues for carbonization management.

4. Conclusions

Different catalyst templates and preparation methods affect the adsorption performance of a catalyst. Molecular sieves and metal–organic frameworks exhibit not only good CO_2 adsorption properties, but also excellent performance in CO_2 conversion into other chemicals. The preparation of catalysts with different functions and selectivity involves adjusting the proportion of different components in the catalyst, introducing functional groups, doping metal ions, and preparing composite materials. In molecular sieve adsorbents, specific surface area and pore structure are the main influencing factors on adsorption performance. MOF adsorbents mainly rely on van der Waals forces to adsorb CO_2, and increasing the specific surface area or alkaline adsorption sites of CO_2 significantly improves the adsorption performance of the adsorbent.

Chemical utilization of CO_2 is an important way to achieve clean utilization of fossil fuels. CO_2 is converted into high-value-added products through thermal catalysis, photocatalysis, and electrocatalysis methods. And its research has important academic value and broad application prospects. From the principles of CO_2 chemistry, catalytic activation, catalyst design, and combined utilization with renewable energy, we can not only solve the technical barriers to industrialization of CO_2 chemical utilization, but also reduce dependence on fossil energy.

Current research has limitations: (1) the research on adsorption performance is not comprehensive enough, and most of it is about the amount of CO_2 adsorption. (2) Most catalysts are still in the laboratory stage, and few are put into large-scale commercial production.

The cost of CO_2 capture and utilization projects varies among different industries due to differences in workflow, maturity of capture technology, initial CO_2 concentration in flue gas, and environmental parameters. In future research, more attention should be paid to the stability, economy, and industry practicality of catalysts to adapt to different capture needs.

Author Contributions: F.R.: writing—original draft preparation; W.L.: supervision. All authors have read and agreed to the published version of the manuscript.

Funding: This research received no external funding.

Data Availability Statement: The data is unavailable due to privacy or ethical restrictions.

Conflicts of Interest: The authors declare no conflict of interest.

References

1. Wang, M.T.; Xu, S.L. Current Status and Latest Progress of Carbon Dioxide Capture Technology. *Contemp. Chem. Ind.* **2016**, *45*, 1002–1005.
2. Zhang, X.; Li, Y.; Ma, Q. Research on the Development of Carbon Capture, Utilization and Storage Technology in China. *Eng. Sci.* **2021**, *23*, 70–80.
3. Olajire Abass, A. Recent progress on the nanoparticles-assisted greenhouse carbon dioxide conversion processes. *J. CO_2 Util.* **2018**, *24*, 522–547. [CrossRef]
4. Zhu, Y.C.; Ding, X.X.; Sun, L. Research progress in the coupling of CO_2/C_2H_4 to prepare acrylic acid and its derivatives. *J. Org. Chem.* **2022**, *42*, 965–977.
5. Jiang, G.D.; Huang, Q.L.; Kenarsari, S.D. A new mesoporousa-mine TiO_2 based-combusion CO_2 capture technology. *Appl. Energy* **2015**, *147*, 214–223. [CrossRef]
6. Xie, H. Application status and research progress of carbon dioxide capture technology. *Chem. Fertil. Des.* **2021**, *59*, 1–9.
7. Li, L. *Study on Ionic Thermosynthesis of Nano and Multi Porous Aluminium Phosphate Molecular Sieves*; Liaocheng University: Liaocheng, China, 2022.
8. Chen, D. *Molecular Dynamics Study on the Effect of Diffusion Behavior in Confined Pores of Molecular Sieves on Product Selectivity*; Wuhan Institute of Technology: Wuhan, China, 2022.

9. Li, J.; Sun, X.; Pan, Y. Application of Oil Shale Molecular Sieve Catalyst: A Review. *Chem. Technol. Fuels Oils* **2022**, *58*, 902–911. [CrossRef]
10. Kosslick, H.; Pitsch, I. Christian Jaeger Improved large mesoporous ordered molecular sieves—Stabilization and acid/base functionalization. *Catal. Today* **2010**, *152*, 54–60. [CrossRef]
11. Barthomeuf, D. Conjugate acid-base pairs in zeolite. *J. Phys. Chem.* **1984**, *88*, 42–45. [CrossRef]
12. Barthomeuf, D. Framework induced basicity in zeolites. *Microporous Mesoporous Mater.* **2003**, *66*, 1–14. [CrossRef]
13. Feng, J.W.; Hu, Y.F. Selective Adsorption Separation of CO_2 and CH4 by SSZ-13 Molecular Screening. *Sci. Technol. Chem. Ind.* **2020**, *28*, 54–60.
14. Wahby, A.; Silvestre-Albero, J.; Sepúlveda-Escribano, A.; Rodríguez-Reinoso, F. CO_2 adsorption on carbon molecular sieves. *Microporous Mesoporous Mater.* **2012**, *164*, 280–287. [CrossRef]
15. Wei, W.; Liu, P.P.; Zhang, S.S. Study on the adsorption performance of amino modified irregular molecular sieves for CO_2. *Chem. Res. Appl.* **2015**, *27*, 1870–1874.
16. Abdelhamid, H.N. Dye encapsulated hierarchical porous zeolitic imidazolate frameworks for carbon dioxide adsorption. *J. Environ. Chem. Eng.* **2020**, *8*, 104008. [CrossRef]
17. Fan, J.; Liu, W.; Zhang, Z.; Xu, T. Preparation of Ag-loaded Modified 13X Molecular Sieve and Study on Its Fuel Adsorption and Desulfurization Performance. *J. Funct. Mater.* **2013**, *44*, 2486–2489.
18. Liu, H. *Direct Hydroxylation of Benzene to Phenol over Titanium Silicalite*; East China Normal University: Shanghai, China, 2014.
19. Feng, X. Progress in the Application of Molecular Sieve Catalysts in China. *Chem. Eng. Des. Commun.* **2018**, *44*, 134.
20. Li, X.; Shen, W.L.; Sun, H. Theoretical studies on carbon dioxide adsorption in cation-exchanged molecular sieves. *RSC Adv.* **2020**, *10*, 32241–32248. [CrossRef]
21. Adsorption of CO_2 on Monovalent Cationic RHO Zeolite. In *Proceedings of the Abstract of the 30th Annual Academic Conference of the Chinese Chemical Society-19th Branch: Quantum and Classical Dynamics in Chemistry*; Chinese Chemical Society: Dalian, China, 2016; Volume 24.
22. Yang, K.Z.; Yang, G.; Wu, J.Y. The publisher does not know the formation and change mechanism of CO_2 adsorption structure in different cationic molecular sieves. *Vac. Cryog.* **2021**, *27*, 535–542.
23. Guo, Y.; Sun, T.; Liu, X.; Ke, Q.; Wei, X.; Gu, Y.; Wang, S. Cost-effective synthesis of CHA zeolites with controllable morphology and size. *Chem. Eng. J.* **2019**, *358*, 331–339. [CrossRef]
24. He, L.M.; Jiang, W.L.; Li, L.C. Research progress in CO_2 adsorption materials. *Petrochem. Technol.* **2022**, *51*, 83–91.
25. Siriwardane, R.; Shen, M.S.; Fisher, E.P.; Poston, J.A. Adsorption of CO_2 on molecular sieves and activated carbon. *Energy Fuels* **2001**, *15*, 279–284. [CrossRef]
26. Gao, J.W.; Chen, Z.K. The Effect of Molecular Sieve Pore Structure on CO_2 Adsorption Performance. *Environ. Prot. Chem. Ind.* **2016**, *36*, 661–665.
27. Wang, Y.Y.; Zhang, Q.; Yu, J.H. Synthesis and CO_2 adsorption performance of multi-level porous NaX molecular sieves. *Chem. J. Chin. Univ.* **2020**, *41*, 616–622.
28. Ma, Y.H.; Zhao, H.L.; Tang, S.J. Synthesis of microporous/mesoporous composite molecular sieves and their adsorption performance for CO_2. *Acta Phys-Chim. Sin.* **2011**, *27*, 689–696.
29. Morali, U.; Demiral, H.; Sensoz, S. Preparation of new carbon molecular sieves for optimized carbon dioxide ad sorp tion and product yield. *New Carbon Mater.* **2020**, *35*, 209–224. [CrossRef]
30. Zhu, Q.L.; Xu, Q. Metal–organic framework composites. *Chem. Soc. Rev.* **2014**, *43*, 5468–5512. [CrossRef]
31. Liu, J.; Benin, A.I.; Furtado, A.M.; Jakubczak, P.; Willis, R.R.; LeVan, M.D. Stability effects on CO_2 adsorption for the DOBDC series of metal–organic frameworks. *Langmuir* **2011**, *27*, 11451–11456. [CrossRef]
32. Sun, X.J.; Wang, C.P.; Pan, X.Y. Application of MOFs based porous carbon materials in gas adsorption and separation. *Sci. Bull.* **2021**, *66*, 3590–3603.
33. Millward, A.R.; Yaghi, O.M. Methane-organic frameworks with exceptionally high capacity for storage of carbon dioxide at room temperature. *J. Am. Chem. Soc.* **2005**, *127*, 17998–17999. [CrossRef]
34. Llewellyn, L.P.; Sandrin, E.B.; Christian, S.; Vimont, A.; Daturi, M.; Hamon, L.; De Weireld, G.; Chang, J.S.; Hong, D.Y.; Kyu Hwang, Y.; et al. High uptakes of CO_2 and CH_4 in mesoporous metal organic frameworks MIL-100 and MIL-101. *Langmuir ACS J. Surf. Colloids* **2008**, *24*, 7245–7250. [CrossRef]
35. Hiroyasu, F.; Nakeun, K.; Go, Y.B.; Aratani, N.; Choi, S.B.; Choi, E.; Yazaydin, A.O.; Snurr, R.Q.; O'Keeffe, M.; Kim, J.; et al. Ultrahigh porosity in metal-organic frameworks. *Science* **2010**, *329*, 424–428.
36. Meng, L.L.; Cheng, H.T.; Xue, D.X. Synthesis and CO_2 selective adsorption properties of a rtl metal organic skeleton material based on 5-(3-aminopyridin-4-yl)-isophthalic acid and paddle wheel shaped [$Cu_2(COO)_4$] clusters. *Chin. J. Inorg. Chem.* **2020**, *36*, 1098–1104.
37. Planas, N.; Dzubak, A.L.; Poloni, R.; Lin, L.C.; McManus, A.; McDonald, T.M.; Neaton, J.B.; Long, J.R.; Smit, B.; Gagliardi, L. The mechanism of carbon dioxide adsorption in an alkylamine-functionalized metal–organic frame work. *J. Am. Chem. Soc.* **2013**, *135*, 7402–7405. [CrossRef] [PubMed]
38. Liu, Q.W. *CO_2 Adsorption Characteristics of Modified Fumaric Acid Based Metal Organic Skeleton Materials*; Chongqing University: Chongqing, China, 2019.

39. Vaidhyanathan, R.; Iremonger, S.S.; Dawson, K.W.; Shimizu, G.K.H. An amine-functionalized metal organic framework for preferential CO_2 adsorption at low pressures. *Chem. Commun.* **2009**, *35*, 5230–5232. [CrossRef] [PubMed]
40. Meng, W.; Zeng, Y.; Liang, Z.; Guo, W.; Zhi, C.; Wu, Y.; Zhong, R.; Qu, C.; Zou, R. Cover Feature: Tuning Expanded Pores in Metal–Organic Frameworks for Selective Capture and Catalytic Conversion of Carbon Dioxide. *Chem. Sus. Chem.* **2018**, *11*, 3691. [CrossRef]
41. Yang, G.Y.; Yu, J.L.; Peng, S.W.; Sheng, K.; Zhang, H. Poly(ionic liquid)-Modified Metal Organic Framework for Carbon Dioxide Adsorption. *Polymers* **2020**, *12*, 370. [CrossRef] [PubMed]
42. Wang, X.G. *Preparation and CO_2 Adsorption Performance of Metal Organic Skeleton Materials MIL-101 and MOF-74*; Dalian University of Technology: Dalian, China, 2018.
43. Park, J.; Yuan, D.; Pham, K.T.; Li, J.-R.; Yakovenko, A.; Zhou, H.-C. Reversible alteration of CO_2 adsorption upon photochemical or thermal treatment in a metal–organic framework. *J. Am. Chem. Soc.* **2012**, *134*, 99–102. [CrossRef]
44. Sun, Y.; Jian, W.; Xie, W.; Tong, S.; Deng, C. Research progress on metal organic skeleton materials for CO_2 adsorption. *Appl. Chem. Ind.* **2021**, *50*, 3482–3488.
45. Cheng, Y. *Preparation of Metal Organic Framework MOF-74 and Its Study on CO_2 Capture*; Xi'an University of Technology: Xi'an, China, 2021.
46. Xiang, Z.; Hu, Z.; Cao, D.; Cao, D.; Yang, W.; Lu, J.; Han, B.; Wen, W. Metal-organic frame works with incorporated carbon nanotubes: Improving carbon-oxide and methane storage capacities by liyhium doping. *Angew. Chem. Int. Ed. Engl.* **2011**, *50*, 491–494. [CrossRef]
47. Yuan, J.; Liu, X.; Li, X.; Yu, J.; Li, X. Computer simulations for the adsorption and separation of $CH_4/H_2/CO_2/N_2$ gases by hybrid ultramicroporous materials. *Mater. Today Commun.* **2021**, *26*, 101987. [CrossRef]
48. Liu, X.; Chen, H.; Yuan, J. Study on the adsorption and separation performance of anionic column hybrid metal organic skeleton materials for N_2/CO_2 [J/OL]. *New Chem. Mater.* **2023**. *prepublish*.
49. Nguyen Phuong, T.K.; Tran, Y.B.N. Copper-Based Metal-Organic Framework for Selective CO_2 Adsoprtion and Catalysis Fixation of CO_2 into Cyclic Carbonates. *Chem. Sel.* **2021**, *6*, 4067–4073.
50. Chen, Y.W. *Preparation of Several Metal Organic Skeleton Materials and Their CO_2 Capture and Olefin Alkane Adsorption and Separation Performance*; South China University of Technology: Guangzhou, China, 2020.
51. Lomig, H.; Jolimaître, E.; Pirngruber, P. CO_2 and CH_4 separation by adsorption using Cu-BTC metal−organic framework. *Ind. Eng. Chem. Res.* **2010**, *49*, 7497–7503.
52. Kim, T.K.; Suh, M.P. Selective CO_2 adsorption in a flexible non-interpenetrated metal–organic framework. *Chem. Commun.* **2011**, *47*, 4258–4260. [CrossRef]
53. Liu, X.B.; Tang, J.F.; Hu, S.Y. Comparative experiments on adsorption and decarbonization of five types of zeolite mo-lecular sieves. *Gas Heat* **2021**, *41*, 19–24+29+45–46.
54. Sun, F.; Wang, C.Y.; Lou, C. CO_2 adsorption characteristics of synthesized NaY zeolite. *J. Clean Coal Technol.* **2021**, *27*, 225–231.
55. Song, X.; Yu, J.; Wei, M.; Li, R.; Pan, X.; Yang, G.; Tang, H. Ionic Liquids-Functionalized Zeolitic Imidazolate Framework for Carbon Dioxide Adsorption. *Materials* **2019**, *12*, 2361. [CrossRef]
56. Liu, L.; Jin, S.; Ko, K.; Kim, H.; Ahn, I.-S.; Lee, C.-H. Alkyl-functionalization of (3-Aminopropyl) triethoxysilane-grafted zeolite beta for carbon dioxide capture in temperature swing adsorption. *Chem. Eng. J.* **2019**, *382*, 122834. [CrossRef]
57. Chang, F.; Zhan, G.X.; Shi, S.S. Evaluation and Analysis of Methanol Synthesis Process by Ionic Liquid Electror eduction of CO_2. *Chem. Ind. Eng. Prog.* **2022**, *41*, 1256–1264.
58. Mohammad, I.O.; Mahdi, N.S.; Federico, G. Photocatalytic carbon dioxide reduction to methanol catalyzed by ZnO, Pt, Au, and Cu nanoparticles decorated zeolitic imidazolate framework-8. *J. CO_2 Util.* **2021**, *43*, 101373.
59. Yin, Z.; Xu, Z.; Li, Y.; Liu, Y.; W, P.; Li, Y.; Zhao, R. Study on the Mechanism of CO_2 Adsorption by Metal Organic Framework NH_2-MIL-101 (Cr). *J. Phys. Chem.* **2021**, *49*, 198–201, 206.
60. Gao, H.; Yan, Y.; Liu, Z.X. Review of large-scale CO_2 removal and utilization technologies. *Pet. Forum* **2011**, *28*, 42–52.
61. Dwarakanath, R.; Keoleian, G.A.; Sick, V. Assessing the Relative Climate Impact of Carbon Utilization for Concrete, Chemical, and Mineral Production. *Environ. Sci. Technol.* **2021**, *5*, 12019–12031.
62. Kong, X.Y.; Xie, L.; Wang, Y.M. CO_2 capture and resource utilization. *Chem. Ind. Eng.* **2022**, *41*, 1187–1198.
63. Lin, Y.; Yue, H.R.; Liu, C.J. Theoretical Calculation of Ag Monoatom Supported N Modified Graphene Catalyzed CO_2 Hydrogenation to Formic Acid. *Chem. Ind. Eng.* **2022**, *40*, 25–32.
64. Guo, L.N.; He, X.B.; Lu, L. Selective Electrocatalytic Reduction of CO_2 to HCOOH by Regulating the Surface Properties of CuO. *J. Inorg. Mater.* **2022**, *37*, 29–37. [CrossRef]
65. He, J.H.; Chang, S.S.; Haoranet, D. Efficient hydrogenation of CO_2 to formic acid over amorphous NiRuB catalysts. *J. CO_2 Util.* **2021**, *54*, 101751. [CrossRef]
66. Asare-Bediako, B.B.; Qian, Q.L.; Wang, Y.; Zhang, J.; Wang, Z.; Li, S.; Liu, H.; Wu, T.; Ge, M.; Han, B. Synthesis of higher carboxylic acids via reaction of polyols with CO_2 and H_2. *Chem Catal.* **2021**, *2*, 114–124. [CrossRef]
67. Zhao, J.W.; Xue, L.; Niu, Z.J.; Huang, L.; Hou, Y.; Zhang, Z.; Yuan, R.; Ding, Z.; Fu, X.; Lu, X.; et al. Conversion of CO_2 to formic acid by integrated all-solar-driven artificial photosynthetic system. *J. Power Sources* **2021**, *512*, 230532. [CrossRef]
68. Rivarolo, M.; Bellotti, D.; Magistrl, L.; Massardo, A. Feasibility study of methanol production from different renewable sources and thermoeconomic analysis. *Int. J. Hydrogen Energy* **2016**, *41*, 2105–2116. [CrossRef]

69. Li, X.; Faghri, A. Development of a direct methanol fuel cell stack fed with pure methanol. *Int. J. Hydrogen Energy* **2012**, *37*, 14549–14556. [CrossRef]
70. Koh, M.K.; Wong, Y.J.; Chai, S.P.; Mohamed, A.R. Carbon dioxide hydrogenation to methanol over multi-functional catalyst: Effects of reactants adsorption and metal-oxide(s)interfacial area. *J. Ind. Eng. Chem.* **2018**, *62*, 156–165. [CrossRef]
71. Chen, D.S.; Xing, H.Z.; Wang, C.Q.; Su, Z. Highly efficient visible-light-driven CO_2 reduction to formate by a new anthracene-based zirconium MOF via dual catalytic routes. *J. Mater. Chem. A* **2016**, *4*, 2657–2662. [CrossRef]
72. Zhang, Y.; Wang, Y.; Tian, Y. Comparative studies on carbon dioxide emissions of typical modern coal chemical processes. *Chem. Ind. Eng. Prog.* **2016**, *35*, 4060–4064.
73. Hsiang, T.I.; Ju, Y.B.; Ya, C.P. Sugarcane bagasse supported graphitic carbon nitride for photocatalytic conversion of carbon dioxide. *Catal. Commun.* **2022**, *164*, 106431.
74. Wang, H. *Study on the Construction, Surface Interface Structure Regulation, and Catalytic Performance of Novel Copper Based Catalysts for CO_2 Hydrogenation to Methanol*; Beijing University of Chemical Technology: Beijing, China, 2021.
75. Wang, L.; Jiang, F.; Xu, Y.B. The effect of Ga additive on Cu@ZnO The Effect of Catalytic CO_2 Hydrogenation on the Performance of Methanol Production. *Chem. Ind. Times* **2021**, *35*, 1–4.
76. Sukhjot, K.; Mukesh, K.; Divyani, G.; Mohanty, P.P.; Das, T.; Chakraborty, S.; Ahuja, S.; Nagaiah, T.C. Efficient CO_2 utilization and sustainable energy conversion via aqueous Zn-CO_2 batteries. *Nano Energy* **2023**, *109*, 108242.
77. Tang, Q.L.; Hong, Q.J.; Liu, Z.P. CO_2 fixation into methanol at Cu/ZrO_2 interface from first principles kinetic Monte Carlo. *J. Catal.* **2009**, *263*, 114–122. [CrossRef]
78. Li, C.F.; Zhong, S.H. Study on application of membrane reactor in direct synthesis DMC from CO_2 and CH_3OH over Cu-KF/MgSiO catalyst. *Catal. Today* **2003**, *82*, 83–90. [CrossRef]
79. Xuan, K.; Chen, S.K.; Pu, Y.F.; Guo, Y.; Guo, Y.; Li, Y.; Pu, C.; Zhao, N.; Xiao, F. Encapsulating phosphotungstic acid within metal-organic framework for direct synthesis of dimethyl carbonate from CO_2 and methanol. *J. CO_2 Util.* **2002**, *59*, 101960. [CrossRef]
80. Rao, V.V.; Krishnamurthi, M. High yield room temperature conversion of carbon dioxide into cyclic carbonates catalyzed by mixed metal oxide (CuO-ZnO) nano-flakes/micro-flakes (Cozi-nmf). *Appl. Organomet. Chem.* **2021**, *35*. [CrossRef]
81. Wu, Y.; Chen, Z.; Zhang, X.; Chen, J.; Wang, Y.; Xu, J. Kinetic study of CO_2 fixation into propylene carbonate with water as efficient medium using microreaction system. *Chin. J. Chem. Eng.* **2022**, *50*, 247–253. [CrossRef]
82. Song, C.F.; Han, X.X.; Yin, Q.R.; Chen, D.; Li, H.; Li, S. Performance intensification of CO_2 absorption and microalgae conversion (CAMC) hybrid system via low temperature plasma (LTP) treatment. *Sci. Total Environ.* **2021**, *801*, 149791. [CrossRef]
83. Goswami, R.K.; Kumar, A.; Mehariya, S.; Milino, A.; Musmarra, D. Microalgae-Based Biorefinery for Utilization of Carbon Dioxide for Production of Valuable Bioproducts. In *Chemo-Biological Systems for CO_2 Utilization*; CRC Press: Boca Raton, FL, USA, 2020; pp. 203–228.
84. Wiesberg, I.L.; Brigago, G.V.; de Medeiros, J.L.; de Queiroz Fernandes Araújo, O. Carbon dioxide utilization in a microalga-based biorefinery: Efficiencyof carbon removal and economic performance under carbontaxation. *J. Environ. Manag.* **2017**, *203*, 988–998. [CrossRef]
85. Chauhan, D.S.; Sahoo, L.; Mohanty, K. Maximize microalgal carbon dioxide utilization and lipid productivity by using toxic flue gas compounds as nutrient source. *Bioresour. Technol.* **2022**, *348*, 126784. [CrossRef]
86. Jing, X.; Jiong, C.; Runtian, H.; Jia, L.; Chun, W.; Heng, Z.; Fang, J. Revealing the GHG reduction potential of emerging biomass-based CO_2 utilization with an iron cycle system. *Front. Environ. Sci. Eng.* **2023**, *17*, 127.
87. Xing, L.; Wu, Z.; Zhang, R. Analysis of the Current Situation and Prospects of CCUS Industry Development. *Int. Pet. Econ.* **2021**, *29*, 99–105.
88. Monkman, S.; MacDonald, M. On carbon dioxide utilization as a means to improve the sustainability of ready-mixed concrete. *J. Clean. Prod.* **2017**, *167*, 365–375. [CrossRef]
89. Kang, D.; Jo, H.; Lee, M.G.; Park, J. Carbon dioxide utilization using a pretreated brine solution at normal temperature and pressure. *Chem. Eng. J.* **2016**, *284*, 1270–1278. [CrossRef]
90. Kumar, R.S.; Sinha, A.S.K.; Sharma, T.; Arif, M. Nanocomposite of binary colloids in effective CO_2 utilization in porous media for enhanced oil production and wettability alteration. *J. Environ. Chem. Eng.* **2023**, *11*, 110442. [CrossRef]
91. Zhuo, L.; Jiang, D.; Weina, M. Achieving low-carbon cementitious materials with high mechanical properties using $CaCO_3$ suspension produced by CO_2 sequestration. *J. Clean. Prod.* **2022**, *373*, 133546.
92. Liu, L.; Liu, Y.; Tian, X.; Chen, X. Superior CO_2 uptake and enhanced compressive strength for carbonation curing of cement-based materials via flue gas. *Constr. Build. Mater.* **2022**, *346*, 128364. [CrossRef]

Disclaimer/Publisher's Note: The statements, opinions and data contained in all publications are solely those of the individual author(s) and contributor(s) and not of MDPI and/or the editor(s). MDPI and/or the editor(s) disclaim responsibility for any injury to people or property resulting from any ideas, methods, instructions or products referred to in the content.